Freeze-Out Conditions in Heavy Ion Collisions from QCD Thermodynamics

A. Bazavov,[1] H.-T. Ding,[1] P. Hegde,[1] O. Kaczmarek,[2] F. Karsch,[1,2] E. Laermann,[2] Swagato Mukherjee,[1] P. Petreczky,[1] C. Schmidt,[2] D. Smith,[2] W. Soeldner,[3] and M. Wagner[2]

[1]*Physics Department, Brookhaven National Laboratory, Upton, New York 11973, USA*
[2]*Fakultät für Physik, Universität Bielefeld, D-33615 Bielefeld, Germany*
[3]*Institut für Theoretische Physik, Universität Regensburg, D-93040 Regensburg, Germany*

(Received 18 August 2012; published 9 November 2012)

We present a determination of freeze-out conditions in heavy ion collisions based on ratios of cumulants of net electric charge fluctuations. These ratios can reliably be calculated in lattice QCD for a wide range of chemical potential values by using a next-to-leading order Taylor series expansion around the limit of vanishing baryon, electric charge and strangeness chemical potentials. From a computation of up to fourth order cumulants and charge correlations we first determine the strangeness and electric charge chemical potentials that characterize freeze-out conditions in a heavy ion collision and confirm that in the temperature range 150 MeV $\leq T \leq$ 170 MeV the hadron resonance gas model provides good approximations for these parameters that agree with QCD calculations on the 5%–15% level. We then show that a comparison of lattice QCD results for ratios of up to third order cumulants of electric charge fluctuations with experimental results allows us to extract the freeze-out baryon chemical potential and the freeze-out temperature.

DOI: 10.1103/PhysRevLett.109.192302 PACS numbers: 25.75.−q, 12.38.Gc, 12.38.Mh, 24.60.−k

Introduction.—A central goal of experiments at the Relativistic Heavy Ion Collider (RHIC) [1] is the exploration of the phase diagram of quantum chromodynamics (QCD) at nonzero temperature (T) and baryon chemical potential (μ_B). In particular, a systematic beam energy scan is being performed at RHIC in order to search for the QCD critical point that has been postulated to exist in the T-μ_B phase diagram of QCD [2,3]. The measurement of fluctuations of conserved charges, e.g., net baryon number (B), electric charge (Q), and strangeness (S) [4–6], plays a crucial role in this search for critical behavior [7] and the exploration of the QCD phase diagram in general.

Fluctuations of conserved charges may reflect thermal conditions at the time where the expanding medium, created during a heavy ion collision, cooled down and diluted sufficiently so that hadrons reappear. It may be questioned whether the thermal medium at this time is in equilibrium and whether hadronization of all species takes place at the same time. However, statistical hadronization models, based on thermal hadron distributions given by the hadron resonance gas (HRG) model, describe the hadronization process quite successfully [8]. Moreover, HRG model calculations of net baryon number fluctuations [9] describe well experimental data on net proton fluctuations [4]. This seems to suggest that at the time of freeze-out the system can be described by thermodynamics characterized by a temperature T_f and a baryon chemical potential μ_B^f.

Conserved charge fluctuations can probe critical behavior if these fluctuations are generated at a point, characterized by (T_f, μ_B^f), close to the QCD transition line and eventually also close to the critical point. The freeze-out points (T_f, μ_B^f) are usually determined by comparing experimental hadron multiplicities with HRG model calculations [8,10]. In order to put these parameters on a firm basis and compare them with the QCD transition line it is desirable to extract the freeze-out parameters by comparing experimental data with a QCD calculation. This requires observables which are experimentally accessible and can also reliably be calculated in QCD. The fluctuations of conserved charges and their higher order cumulants are such observables. Experimentally, net baryon number fluctuations are accessible only through net proton number fluctuations [4], inaccessible to lattice QCD (LQCD). We thus focus on the net electric charge fluctuations.

We present lattice calculations of ratios formed out of the first three cumulants, i.e., mean (M_X), variance (σ_X^2), and skewness (S_X) of the net charge distributions $X = B$, Q, and S. They can be used to extract (T_f, μ_B^f) from corresponding experimental measurements.

Strangeness and electric charge chemical potentials.—To access (T_f, μ_B^f) we need to fix the electric charge (μ_Q) and strangeness (μ_S) chemical potentials characterizing the thermal system created during heavy ion collisions. They are determined assuming the thermal subvolume, probed by measuring fluctuations in a certain acceptance window, reflects the net strangeness content and electric charge to baryon number ratio of the incident nuclei,

$$M_S \equiv 0, \qquad M_Q = rM_B, \tag{1}$$

where $M_X = (VT^3)^{-1}\partial \ln Z(\mu, T)/\partial \hat{\mu}_X$ is the expectation value of the density of net charge X, $\mu = (\mu_B, \mu_Q, \mu_S)$

summarizes the three charge chemical potentials, and $\hat{\mu}_X \equiv \mu_X/T$. At any value of (T, μ_B) the chemical potentials (μ_Q, μ_S) satisfying these constraints can be evaluated in QCD. We perform Taylor expansions of the densities M_X in terms of the three chemical potentials and calculate the expansion coefficients of this series using LQCD. This involves the numerical calculation of generalized susceptibilities (In the following, subscripts and the corresponding superscripts are suppressed in cases where the former is zero; furthermore the abbreviation $\chi^{BQS}_{ijk} = \chi^{BQS}_{ijk,\mu=0}$ is used.) [11]

$$\chi^{BQS}_{ijk,\mu} = \frac{1}{VT^3} \frac{\partial^{i+j+k} \ln Z(\mu, T)}{\partial \hat{\mu}_B^i \partial \hat{\mu}_Q^j \partial \hat{\mu}_S^k}, \tag{2}$$

at $\mu = 0$. Recent LQCD calculations [12,13] provide continuum extrapolated results for the susceptibilities needed to determine $(\hat{\mu}_Q, \hat{\mu}_S)$ to leading order (LO) in $\hat{\mu}_B$.

Let us write the next-to-leading order (NLO) expansion of $\hat{\mu}_Q$ and $\hat{\mu}_S$ as $\hat{\mu}_Q = q_1 \hat{\mu}_B + q_3 \hat{\mu}_B^3$, $\hat{\mu}_S = s_1 \hat{\mu}_B + s_3 \hat{\mu}_B^3$. Expanding the densities M_X up to third order in the chemical potentials, we can fulfill the constraints specified in Eq. (1) at NLO. This provides four equations to determine the four parameters (s_1, s_3, q_1, q_3). In LO, one obtains,

$$\begin{aligned} q_1 &= \frac{r(\chi^B_2 \chi^S_2 - \chi^{BS}_{11}\chi^{BS}_{11}) - (\chi^{BQ}_{11}\chi^S_2 - \chi^{BS}_{11}\chi^{QS}_{11})}{(\chi^Q_2 \chi^S_2 - \chi^{QS}_{11}\chi^{QS}_{11}) - r(\chi^{BQ}_{11}\chi^S_2 - \chi^{BS}_{11}\chi^{QS}_{11})}, \\ s_1 &= -\frac{\chi^{BS}_{11}}{\chi^S_2} - \frac{\chi^{QS}_{11}}{\chi^S_2} q_1. \end{aligned} \tag{3}$$

The NLO expressions can be derived easily [14]. We evaluated the LO expressions in the temperature interval 150 MeV $\leq T \leq$ 250 MeV for three different values of the lattice cutoff (a) corresponding to lattices with temporal extent $N_\tau \equiv 1/aT = 6$, 8, and 12. All calculations have been performed within an $\mathcal{O}(a^2)$ improved gauge and staggered fermion (highly improved staggered quark) discretization scheme [15] for $(2 + 1)$ flavor QCD using a strange quark mass tuned to its physical value and the light to strange quark mass ratio $m_l/m_s = 1/20$, leading to a Goldstone pion mass of about 160 MeV. For LO results we make use of data obtained by the HotQCD collaboration [12]. On the $24^3 \times 6$ and $32^3 \times 8$ lattices we extended these calculations in the temperature interval 150 MeV $\leq T \leq$ 175 MeV to 30 000 molecular dynamics time units.

In the following, we restrict our discussion to the case $r = 0.4$, which approximates well the situations met in Au-Au as well as Pb-Pb collisions. The LO expansion coefficients for $(\hat{\mu}_Q, \hat{\mu}_S)$ are shown in the top panels of Fig. 1, left and middle panels. Using spline interpolations of results for three different lattice sizes, we performed continuum extrapolations shown as bands, using an ansatz linear in $1/N_\tau^2$. No statistically significant differences occur by including an additional $1/N_\tau^4$ correction.

To check the importance of NLO corrections we have calculated s_3 and q_3 on $N_\tau = 6$ and 8 lattices. As shown in Fig. 1, NLO corrections are negligible in the high temperature region and are below 10% in the relevant temperature interval $T \simeq (160 \pm 10)$ MeV. In this temperature range, leading order LQCD results deviate from HRG model calculations expanded to the same order by less than 15%. The NLO corrections become smaller than the HRG model values for $T \gtrsim 160$ MeV, further reducing the importance of NLO corrections. In the HRG model, the NLO expansion reproduces the full HRG result for $(\hat{\mu}_Q, \hat{\mu}_S)$ to better than 1.0% for $\mu_B/T \leq 1.3$. We thus expect that the NLO expansion is a good approximation to the complete results for $(\hat{\mu}_Q, \hat{\mu}_S)$ for $\mu_B \leq 200$ MeV.

As our study utilizes the staggered discretization scheme the biggest systematic effects at nonvanishing lattice spacing are due to so-called taste violations, giving rise to a distorted hadron spectrum, but mainly affecting the

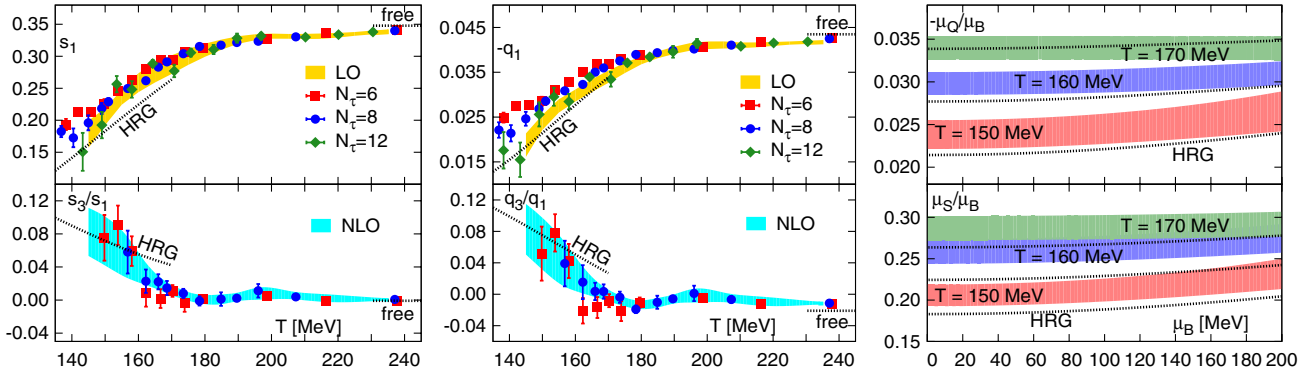

FIG. 1 (color online). The leading and next-to-leading order expansion coefficients of the strangeness (left panel) and the negative of the electric charge chemical potentials (middle panel) versus temperature for $r = 0.4$. For s_1 and q_1 the LO bands show results for the continuum extrapolation. For s_3 and q_3 we give an estimate for continuum results (NLO bands) based on spline interpolations of the $N_\tau = 8$ data. Dashed lines at low temperature are from the HRG model and at high temperature from a massless, 3-flavor quark gas. The right hand panel shows NLO results for μ_S/μ_B and μ_Q/μ_B as a function of μ_B for three values of the temperature.

pion sector [12]. Correspondingly, the electric charge susceptibilities will be most sensitive to discretization effects while the baryon and strangeness sectors are largely unaffected. At LO, these discretization effects have been eliminated by taking the continuum limit. At NLO, taste violation effects show up in the electric charge sector, Fig. 1 (middle panel). However, as the corrections themselves are already small, we expect their influence to be small. Furthermore, the taste violations can be modelled within the HRG model by replacing the pion mass with the average, root-mean-square pion mass [12]. Results obtained with such a modified spectrum suggest that taste violation effects are indeed negligible in the NLO calculation of $\hat{\mu}_S$ and lead to at most 5% systematic errors in $\hat{\mu}_Q$ for $\mu_B \leq 200$ MeV.

Additional systematic errors arise from the degeneracy of light quark masses. As a consequence, not all susceptibilities are independent; there are two constraints in LO ($\chi_2^B = 2\chi_{11}^{BQ} - \chi_{11}^{BS}$, $\chi_2^S = 2\chi_{11}^{QS} - \chi_{11}^{BS}$) and six constraints in NLO [14]. Imposing these constraints by hand in the HRG model calculations we find that q_1 and q_3 can change by up to 3% while modifications of s_1 and s_3 are below the 1% level. This suggests that even after extrapolating to the continuum limit, the current LQCD calculations of μ_Q/μ_B do have an inherent systematic error of about 3%.

Our results for μ_S and μ_Q at NLO are shown in Fig. 1 (right panel). While μ_S/μ_B varies between 0.2 and 0.3 in the interval 150 MeV $\leq T \leq$ 170 MeV, the absolute value of μ_Q/μ_B is an order of magnitude smaller. Both ratios are almost constant for $\mu_B \leq 200$ MeV, consistent with HRG model calculations.

Ratios of cumulants of net charge fluctuations.—We now evaluate cumulants of net charge fluctuations as a function of T and μ_B for $\mu_S \neq 0$ and $\mu_Q \neq 0$ obeying Eq. (1). As ratios of cumulants, $R_{nm}^X = \chi_{n,\mu}^X/\chi_{m,\mu}^X$, cancel the freeze-out volume we concentrate on such ratios,

$$R_{12}^X \equiv \frac{M_X}{\sigma_X^2} = \hat{\mu}_B(R_{12}^{X,1} + R_{12}^{X,3}\hat{\mu}_B^2 + \mathcal{O}(\hat{\mu}_B^4)), \quad (4)$$

$$R_{31}^X \equiv \frac{S_X\sigma_X^3}{M_X} = R_{31}^{X,0} + R_{31}^{X,2}\hat{\mu}_B^2 + \mathcal{O}(\hat{\mu}_B^4), \quad (5)$$

with $X = B$, Q. These ratios can be calculated in QCD as well as in the HRG model [7], and eventually can be compared to experimental data to determine $(T_f,\ \mu_B^f)$. We evaluated them up to $\mathcal{O}(\hat{\mu}_B^3)$ in a Taylor expansion for R_{12}^X and to LO for R_{31}^X.

Using $\chi_{11}^{XX} \equiv \chi_2^X$ the LO coefficients of the odd-even ratios R_{12}^X can be written as

$$R_{12}^{X,1} = \frac{\chi_{11}^{BX}}{\chi_2^X} + q_1\frac{\chi_{11}^{XQ}}{\chi_2^X} + s_1\frac{\chi_{11}^{XS}}{\chi_2^X}, \quad (6)$$

with $X = B$, Q. They have been evaluated on lattices with temporal extent $N_\tau = 6$, 8, and 12 and have been extrapolated to the continuum limit in the same way as for q_1 and s_1, see Fig. 2 (left panel). In Fig. 2 (right panel), we show the NLO corrections from $N_\tau = 6$ and 8 lattices. The NLO corrections are below 10%, making the LO result a good approximation for a large range of $\hat{\mu}_B$. Systematic errors arising from the NLO truncation for R_{12}^Q may again be estimated by comparing the full result in the HRG model calculation with the corresponding truncated results. For $T = (160 \pm 10)$ MeV and $\mu_B/T \leq 1.3$ we find that the difference is less than 1.0%. Moreover, we estimated that taste violation effects in the NLO calculation lead to systematic errors that are at most 5%. Taylor series truncated at NLO are thus expected to give a good approximation to the full result for a wide range of μ_B.

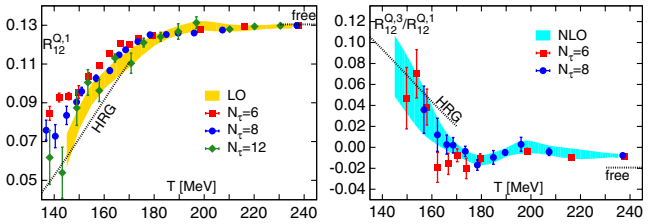

FIG. 2 (color online). The leading (left) and next-to-leading (right panel) order expansion coefficients of the ratio of first to second order cumulants of net electric charge fluctuations versus temperature for $r = 0.4$. The bands and lines are as in Fig. 1 (left panel).

Determination of freeze-out baryon chemical potential and temperature.—The ratio R_{12}^Q shows a strong sensitivity on μ_B but varies little with T for $T \simeq (160 \pm 10)$ MeV. Figure 3 (left panel) shows this ratio as a function of $\hat{\mu}_B$ up to NLO corrections. For the determination of $(T_f,\ \mu_B^f)$, a second, complimentary information is needed. To this end, we use information from the ratio R_{31}^Q, which is strongly dependent on T but receives corrections only at $\mathcal{O}(\hat{\mu}_B^2)$. The LO result for this ratio is shown in Fig. 3 (middle panel). Apparently, this ratio shows a characteristic temperature dependence for $T \gtrsim 155$ MeV that is quite different from that of HRG model calculations. The NLO correction to R_{31}^Q is below 1% in the high temperature free gas limit. At low T, the HRG model suggests that LO contributions to R_{31}^Q differ by less than 2% from the exact results for $\mu_B \leq 200$ MeV. In the transition region a preliminary 6th order calculation at $T = 162$ MeV [14] suggests that the μ_B^2 correction in units of the LO term is $-0.03(10)$. Based on these estimates we expect the NLO corrections to be at most 10% for the whole temperature range. In Fig. 3 (middle panel) we show the spline interpolation for the $N_\tau = 8$ data as a band, and added on top of this, a band that estimates the effect of a 10% contribution of the NLO correction. The ratio R_{31}^Q thus seems to be well suited for a determination of the freeze-out temperature T_f.

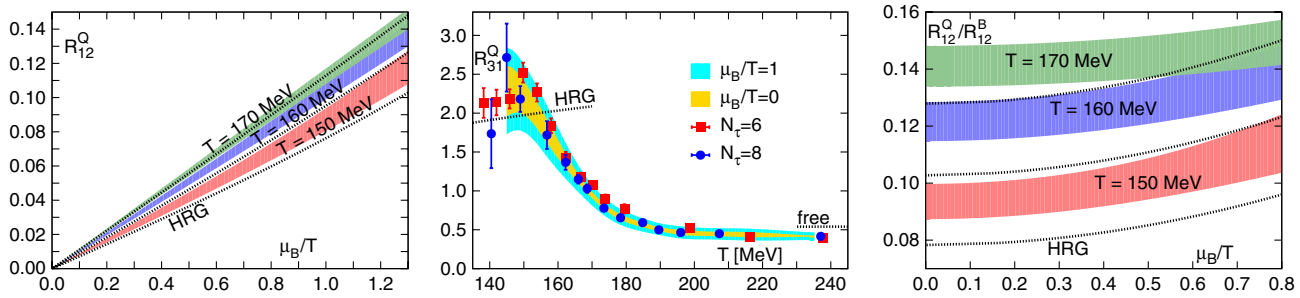

FIG. 3 (color online). The ratios R_{12}^Q versus μ_B/T (left panel) for three values of the temperature and R_{31}^Q versus temperature for $\mu_B = 0$ (middle panel). The wider band on the data set for $N_\tau = 8$ (middle panel) shows an estimate of the magnitude of NLO corrections. The right hand panel shows the NLO result for the ratio of ratios of net electric charge and baryon number fluctuations, respectively.

We now are in a position to extract μ_B^f and T_f from R_{12}^Q and R_{31}^Q which eventually will be measured in the beam energy scan at RHIC. A large value for R_{31}^Q, i.e., $R_{31}^Q \simeq 2$ would suggest a low freeze-out temperature ($T_f \lesssim 155$ MeV), while a value $R_{31}^Q \simeq 1$ would suggest a large freeze-out temperature ($T_f \sim 170$ MeV). A value of $R_{31}^Q \simeq 1.5$ would correspond to $T_f \sim 160$ MeV. A measurement of R_{31}^Q thus suffices to determine T_f. In the HRG model parametrization of the freeze-out curve [10], the favorite value for T_f in the beam energy range 200 GeV $\geq \sqrt{s_{NN}} \geq 39$ GeV varies by less than 2 MeV and is about 165 MeV. At this temperature the values for R_{31}^Q calculated in the HRG model and in QCD differ quite a bit, as is obvious from Fig. 3. While $R_{31}^Q \simeq 2$ in the HRG model, one finds $R_{31}^Q \simeq 1.2$ in QCD at $T = 165$ MeV. Values close to the HRG value are compatible with QCD calculations only for $T \lesssim 157$ MeV. We thus expect to either find freeze-out temperatures that are about 5% below HRG model results or values for R_{31}^Q that are significantly smaller than the HRG value. A measurement of this cumulant ratio at RHIC thus will allow us to determine T_f and probe the consistency with HRG model predictions.

For any of these temperature values a comparison of an experimental value for R_{12}^Q with Fig. 3 (left) will allow us to determine μ_B^f. To be specific, let us discuss the results obtained at $T = 160$ MeV. Here we find: $R_{12}^Q(T = 160\ \text{MeV}) = 0.102(5)\hat{\mu}_B + 0.002(1)\hat{\mu}_B^3$. For a value of the freeze-out temperature close to $T_f = 160$ MeV we thus expect to find $\mu_B^f = (20\text{–}30)$ MeV, if R_{12}^Q lies in the range 0.012–0.020, $\mu_B^f = (50\text{–}70)$ MeV for $0.032 \leq R_{12}^Q \leq 0.045$, and $\mu_B^f = (80\text{–}120)$ MeV for $0.05 \leq R_{12}^Q \leq 0.08$. These parameter ranges are expected [1,10,16] to cover the regions relevant for RHIC beam energies $\sqrt{s_{NN}} = 200$, 62.4, and 39 GeV, respectively. As is evident from Fig. 3 (left panel) the values for μ_B^f will shift to smaller (larger) values when T_f turns out to be larger (smaller) than 160 MeV. A more refined analysis of (T_f, μ_B^f) will become possible, once the ratios R_{12}^Q and R_{31}^Q have been measured experimentally.

Conclusions.—We have shown that the first three cumulants of net electric charge fluctuations are well suited for a determination of freeze-out parameters in a heavy ion collision. Although the ratios R_{12}^Q and R_{31}^Q are sufficient to determine T_f and μ_B^f, it will clearly be advantageous to have several ratios to probe the consistency of an equilibrium thermodynamic description of cumulant ratios at the time of freeze-out. In particular, the ratio of ratios $R_{12}^Q/R_{12}^B = r\chi_{2,\mu}^B/\chi_{2,\mu}^Q$ is also well determined in LQCD calculations [12]. In Fig. 3 (right panel), we show the NLO result for this quantity for $T = (160 \pm 10)$ MeV. Its measurement will not only test our basic assumptions on constraining the electric charge and strangeness chemical potentials, but also constrain possible differences in cumulant ratios of net proton and net baryon number fluctuations. Once the ratios of lower order cumulants have been used to fix the freeze-out parameters, the calculation of higher order cumulants is parameter free and provides unique observables for the discussion of possible signatures for critical behavior along the freeze-out line.

While the calculations presented here have been performed using the grand-canonical ensemble approach in the thermodynamic limit, it is *a priori* not evident that this is also applicable to conditions met in a heavy ion collision. Thus, when comparing our results with experimental ones it is essential to check that effects of global conservation laws in finite subsystem sizes [17], experimental acceptance cuts [18], or the influence of resonance decays [19] do not invalidate the grand canonical ensemble approach. Although many of these questions are being investigated in recent experimental analyses [19,20], clearly these issues deserve further detailed considerations.

We thank P. Bialas, T. Luthe, and L. Wresch for discussions and help with the software development for the Bielefeld GPU cluster. Numerical calculations have also been performed on the USQCD GPU-clusters at JLab and NYBlue at the NYCCS. This work has been supported in part by Contract No. DE-AC02-98CH10886 with the

U.S. Department of Energy, the Bundesministerium für Bildung und Forschung under Grant No. 06BI9001, and the Gesellschaft für Schwerionenforschung under Grant No. BILAER.

[1] B. Mohanty (STAR Collaboration), J. Phys. G **38**, 124023 (2011).
[2] M. Asakawa and K. Yazaki, Nucl. Phys. **A504**, 668 (1989).
[3] J. Berges and K. Rajagopal, Nucl. Phys. **B538**, 215 (1999); M. A. Halasz, A. D. Jackson, R. E. Shrock, M. A. Stephanov, and J. J. M. Verbaarschot, Phys. Rev. D **58**, 096007 (1998).
[4] M. M. Aggarwal *et al.* (STAR Collaboration), Phys. Rev. Lett. **105**, 022302 (2010).
[5] A. Adare *et al.* (PHENIX Collaboration), Phys. Rev. C **78**, 044902 (2008).
[6] B. Abelev *et al.* (ALICE Collaboration), arXiv:1207.6068v1.
[7] S. Ejiri, F. Karsch, and K. Redlich, Phys. Lett. B **633**, 275 (2006).
[8] P. Braun-Munzinger, K. Redlich, and J. Stachel, in *Quark Gluon Plasma*, edited by R. C. Hwa (World Scientific, Singapore, 1990), pp. 491–599.
[9] F. Karsch and K. Redlich, Phys. Lett. B **695**, 136 (2011); P. Braun-Munzinger, B. Friman, F. Karsch, K. Redlich, and V. Skokov, Phys. Rev. C **84**, 064911 (2011).
[10] J. Cleymans, H. Oeschler, K. Redlich, and S. Wheaton, Phys. Rev. C **73**, 034905 (2006).
[11] R. V. Gavai and S. Gupta, Phys. Rev. D **68**, 034506 (2003); C. R. Allton, M. Döring, S. Ejiri, S. J. Hands, O. Kaczmarek, F. Karsch, E. Laermann, and K. Redlich, Phys. Rev. D **71**, 054508 (2005); M. Cheng *et al.*, Phys. Rev. D **79**, 074505 (2009).
[12] A. Bazavov *et al.* (HotQCD Collaboration), Phys. Rev. D **86**, 034509 (2012); A. Bazavov *et al.* (HotQCD Collaboration), Phys. Rev. D **85**, 054503 (2012).
[13] S. Borsanyi, Z. Fodor, S. D. Katz, S. Krieg, C. Ratti, and K. Szabó, J. High Energy Phys. 01 (2012) 138.
[14] Bielefeld-BNL Collaboration (to be published).
[15] E. Follana, Q. Mason, C. Davies, K. Hornbostel, G. Lepage, J. Shigemitsu, H. Trottier, and K. Wong (HPQCD and UKQCD Collaborations), Phys. Rev. D **75**, 054502 (2007).
[16] B. I. Abelev *et al.* (STAR Collaboration), Phys. Rev. C **79**, 034909 (2009).
[17] A. Bzdak, V. Koch, and V. Skokov, arXiv:1203.4529.
[18] A. Bzdak and V. Koch, arXiv:1206.4286.
[19] X. Luo, (STAR Collaboration), arXiv:1210.5573.
[20] J. T. Mitchell (PHENIX Collaboration), in The XXIII International Conference on Ultrarelativistic Nucleus-Nucleus Collisions, Washington D.C., August 13-18, 2012 (to be published); D. McDonald, (STAR Collaboration), arXiv:1210.7023.